Advances in Machinery, Materials Science and Engineering Application X
M. Giorgetti et al. (Eds.)

doi:10.3233/ATDE240690

Design of Intake Tower Structure Based on Elastic Stress Diagram Method

Yi HUANG [a,b], Diqiu LU [b,1], Dabin XU [a] and Guilin DU [a]
[a] Chengdu Engineering Corporation Limited, Power China, Chengdu, 611100, China
[b] Sichuan Municipal Water Environment Management Engineering Technology Research Center, Chengdu, 611100, China

Abstract. In the building of hydro-power station, the inlet tower structure of the spillway tunnel is an important building to ensure the realization of the flood discharge function of the hydro-power station. The tower inlet is a tower-shaped junction against the bank slope. The shaft type water inlet is a gate arranged in the shaft, which is generally suitable for the part of the bank slope is slow and the inlet section has good conditions for forming holes. In this project, the slope of the water inlet is steep and the topographic elevation is low. If the shaft intake is used, there is no condition for the layout of the shaft, and the position of the shaft is close to the left dam abutment, which conflicts with the layout of the dam, so the inlet type is chosen as the tower type. In order to study the rationality and seismic resistance of the design of the intake tower of a hydro-power station preferably, the numerical simulation of the intake tower is carried out based on the finite element analysis method. At the same time, the vertical stress and maximum principal stress of the typical position of the intake tower under two working conditions are given. The calculation results show that the stability of the intake tower is good and the design of the intake tower is reasonable, which provides a scientific basis for the design and construction of the intake water tower and similar research.

Keywords. Intake tower, elastic stress, hydrodynamic pressure, numerical simulation

1. Introduction

The ground cover is crumpling silty clay with crushed rocks [1]. The cover layer in the inlet section is deep [2]. According to the drilling, the thickness of the cover layer is 15 -35m, and the thickness of the cover layer below the tunnel floor is 5-12m. The underlying bedrock is gray-purple calcareous silty mudstone with tigskin grained sandy marl and yellow calcareous mudstone. The rock formation is N15~25° E/SE∠32~43°. During the excavation of the entrance, the overburden had fallen below 1960m. After cutting the slope and strengthening the retaining wall, the slope is now in a stable state. The reconstruction design is as follows: a new bank tower water inlet is built at the entrance position, and C30 reinforced concrete is used to pour, the length of lock chamber section is 6.0m, the slope of the bottom plate is 0, the bottom plate elevation is

[1] Diqiu LU, Corresponding author, Sichuan Municipal Water Environment Management Engineering Technology Research Center, Chengdu, 611100, China; E-mail: p2022076@chidi.com.cn.

1942.50m, and the tower top elevation is 1973.50m. The water intake tower is a square cylinder with a length of 10.0m and a width of 6.6m.

The three-dimensional static and dynamic calculation model of water intake was established based on the structure layout of water intake tower [2]. In the model, solid unit is used to simulate the foundation and concrete structure, and shell unit is used to simulate the machine room and transverse wall in the water intake tower [3]. The semi-infinite foundation and rock slope are simulated according to the traditional massless foundation model to avoid the influence of seismic wave reflection on the structure and the amplification of seismic effect by the foundation [4]. The finite element grid diagram of the water intake tower structure is shown in figure 1.

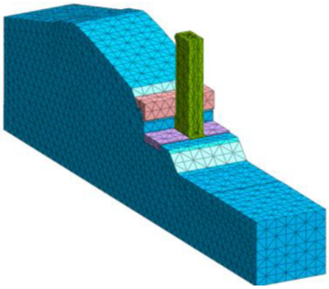

Figure 1. Schematic diagram of a numerical model.

2. Load Calculation Method

2.1. Hydrodynamic Pressure Calculation

When the pseudo-static method is used to calculate the seismic effect of water intake tower [5], the representative value of dynamic water pressure can be directly calculated according to the formula (1).

$$F_T(h) = a_h \xi \rho_w \psi(h) \eta_w A \left(\frac{a}{2H_0} \right)^{-0.2} \tag{1}$$

Where: Ft(h) is water depth h unit height tower surface hydrodynamic pressure representative value [6]. *Ψ(h)* Is the distribution coefficient of dynamic water pressure at water depth *h* shall be 0.72 for the dynamic water pressure inside the tower and the value of the dynamic water pressure outside the tower shall be specified in table 1.

Table 1. Rectangular tower external shape factor.

h/H_0	Ψ(h)	h/H_0	Ψ(h)
0.0	0.00	0.3	0.79
0.1	0.68	0.4	0.70
0.2	0.82	0.5	0.60
0.6	0.48	0.9	0.20
0.7	0.37	1.0	0.17
0.8	0.28		

The representative value of the resultant dynamic water pressure acting on the whole tower surface [7] is calculated according to formula (2), and its application point is at the water depth of $0.42H_0$ [8].

$$F_T = 0.5a_h \xi \rho_w \eta_w A H_0 \left(\frac{a}{2H_0}\right)^{-0.2} \tag{2}$$

2.2. Horizontal Seismic Inertia Force

In general, the seismic action should be considered in the seismic calculation of hydraulic buildings: seismic inertia force generated by the building's own weight and the load on it [9], seismic dynamic earth pressure and ground motion water pressure, and the ground motion pore water pressure should be considered [10].

When the pseudo-static method is used to calculate the seismic effect [11], the representative value of the horizontal seismic inertia force acting on particle *i* along the building height should be calculated according to equation (3)

$$E_i = a_h \xi G_{Ei} \alpha_i / g \tag{3}$$

Where formula is:

E_i is the value of the horizontal seismic inertia force acting on particle *i.*

ζ is the value of the effect reduction factor of seismic action shall be 0.25 unless otherwise specified [12].

G_{Ei} is concentrated on the standard value of gravity action of particle *i*.

a_i is dynamic distribution coefficient of seismic inertia force of particle *i* shall be adopted in accordance with the relevant provisions in the section of various hydraulic structures of code [13].

When the water depth in front and back of the tower is different, the representative value of the dynamic water pressure or the representative value of the additional mass at each elevation can be calculated according to the two water depths respectively. The ratio of the average width of the facing water surface perpendicular to the direction of earthquake action to the maximum water depth in front of the tower group connected in a row. When a/H is greater than 3.0, the external dynamic water pressure per unit height at water depth h can be calculated according to the resultant force of pseudo-static method and the additional mass of dynamic method respectively.

3. Analysis of Calculation Results

3.1. Numerical Calculation Results of Tower

Figures 2-5 show the maximum stress and displacement mode of the tower under quasi-static seismic action. The tower body is a narrow-height towering structure with small horizontal stiffness, among which the vertical flow stiffness is the least. Therefore, the control condition is dominated by horizontal seismic action in the vertical flow direction and horizontal tensile stress in the main foundation structure in the downstream flow direction. Considering that the column body is constrained by water pressure on three sides, the left and right sides of the column body do not have large tension and deformation.

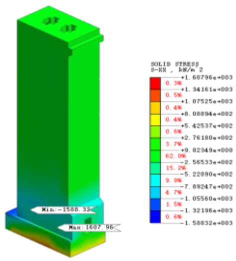

Figure 2. X direction tower body stress diagram.

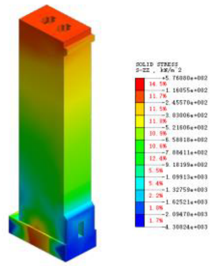

Figure 3. Z direction tower body stress diagram.

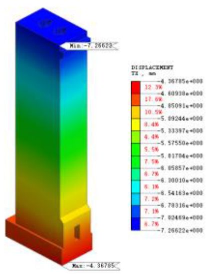

Figure 4. X shift the tower displacements (mm).

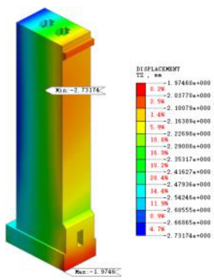

Figure 5. Z shift the tower displacements (mm).

3.2. Elastic Stress Diagram Method

Non-bar system reinforced concrete structure refers to the reinforced concrete structure in which the internal force of the section cannot be calculated according to the mechanical method of the bar structure. For the non-bar system reinforced concrete structure with no significant change in stress state before and after solidification, the amount of reinforcement required for the calculation of bearing capacity can be determined by the graph area of elastic principal tensile stress obtained by the elastic theory analysis method. For the non-bar system reinforced concrete structures with significant changes in stress state before and after coagulation cracking, the amount of reinforcement required is determined according to the area of elastic principal tensile stress figure, and the finite element method of reinforcement coagulation should be used to check [14].

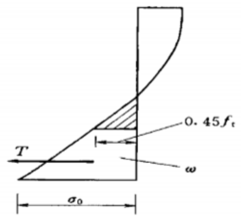

Figure 6. Elastic stress reinforcement diagram.

When the height of the tension zone of the elastic stress figure is greater than 2/3 of the height of the transverse plane of the structure, the cross-sectional area of the tension steel bar should be calculated according to the full area of the square projection figure of the elastic principal tension force [15].

$$A_s \geq \frac{KT}{f_y} \tag{4}$$

4. Conclusions and Recommendations

(1) The main tensile force of the section is deposited on the total surface of the projection pattern in the direction of the reinforcement except that the tensile force value is less than the surface area of the figure after 0.45 f_t (N/mm), but the area of the subtracted parts (as shown in the shaded part in figure 6) should not exceed 30% of the total surface area, where, f_t is the value of axial tensile strength of concrete (N/mm).

(2) When the tensile zone height of the elastic stress figure is less than 2/3 of the height of the structure cross-section, and the maximum tensile stress of the section edge is not more than 0.45ft, only the structural steel bar can be installed. The configuration of the reinforcement should be determined according to the stress figure and the stress point of the structure. When the reinforcement is mainly controlled by load bearing force and the structure has obvious bending and breaking characteristics, the tension reinforcement can be arranged on the edge of the tension zone.

(3)When the reinforcement is mainly controlled by the crack width, the reinforcement can be arranged in layers within a wide range of tensile stress, and the number of reinforcement layers should correspond to the distribution of tensile stress patterns. When checking the crack width, it is advisable to use the non-linear finite element sequence of steel reinforced concrete to directly obtain the distribution and width of the crack.

References

[1] Gogus M, et al. Experimental investigation of the anti-vortex devices of beyhan 1 dam and hydroelectric power plant water intake structure. Procedia Engineering. 2016; 161: 881-886.

[2] Pan J, et al. Influence of intake port structure on the performance of a spark-ignited natural gas engine. Energies. 2022; 15(22): 8545.

[3] Andrey LP, et al. Telescopic water intake with stilling well. Magazine of Civil Engineering. 2022; 112(4): 173.

[4] Gregor Z and Gregor L. Experimental hydraulic analysis of intake structure for cooling towers pumps. Strojniski Vestnik/ Journal of Mechanical Engineering. 2018; 64(9): 566-576.

[5] Gabl, R, et al. Adaptation of an existing intake structure caused by increased sediment level. Water (Switzerland). 2018; 10(8): 1066.

[6] Liu HD, et al. Numerical analysis of flow field and aerodynamic noise in intake structure. Journal of Physics: Conference Series. 2023; 2463(1).

[7] Xu CD, et al. Three-dimensional reverse modeling and hydraulic analysis of the intake structure of pumping stations on sediment-laden rivers. Water Resources Management. 2023; 37(1): 537-555.

[8] Pei TY, Chen FX, et al. Research on the intake port of a uniflow scavenging GDI opposed-piston two-stroke engine. Energies. 2022; 15(6): 2148.

[9] Halilovič M, et al. Prediction of recirculation flow rate for icing prevention in water intake supply systems of nuclear power plants. Cold Regions Science and Technology. 2019; 161: 63-70.

[10] Chen X, et al. Seismic response analysis of intake tower structure under near-fault ground motions with forward-directivity and fling-step effects. Soil Dynamics and Earthquake Engineering. 2020; 132: 106098.

[11] Ma Z, et al. Flow characteristics and power generation effect of a seawater intake caisson integrated with a wave-energy converter. Journal of Waterway, Port, Coastal and Ocean Engineering. 2023; 149(3): 04023001.

[12] Huang Y, Li L, Ma Y, Cheng L, Yan R. Research on failure treatment of anchor cable anti slide pile based on 3D modeling and artificial intelligence reduction algorithm. Proceedings of 2022 International Conference on Applied Physics and Computing, ICAPC, 2022; p. 341-344.

[13] Huang Y, et al. Study on failure mechanism of pebble slope based on nonsynchronous double strength reduction method. IOP Conference Series: Earth and Environmental Science. 2021; 861(6), p. 062018.

[14] Huang Y, et al. Dynamic response analysis of pile group foundation of super-giant sewage treatment structure on hydraulic fill foundation. Shock and Vibration. 2022.

[15] Shay N, Mark T and Sam F. Swelling of compacted clay as affected by quantity of water intake and soil structure. Geotechnical and Geological Engineering. 2022; 40(10): 4961-4974.